

Influence of Tunnel Geometry and Environmental Factors on Fire Smoke Characteristics under a Blowing–Suction Air Curtain



Yang Xu^{*}, Mengnan Kou^{}, Xiaoyan Li^{}

School of Smart Energy and Environment, Zhongyuan University of Technology, Zhengzhou 450007, China

Corresponding Author Email: xy19851923923@163.com

Copyright: ©2026 The authors. This article is published by IIETA and is licensed under the CC BY 4.0 license (<http://creativecommons.org/licenses/by/4.0/>).

<https://doi.org/10.18280/ijht.440119>

ABSTRACT

Received: 10 September 2025

Revised: 10 January 2026

Accepted: 19 January 2026

Available online: 28 February 2026

Keywords:

twin fire sources, tunnel cross-sectional size, longitudinal wind speed, ambient temperature and humidity

With the anticipated increase in traffic volume, tunnel construction is trending toward larger cross-sections and expansion into extreme environmental conditions. This study employs the Fire Dynamics Simulator (FDS) to investigate the effects of tunnel cross-sectional size, longitudinal wind speed, ambient temperature, and humidity on smoke behavior in a twin-fire scenario under the action of a blowing–suction air curtain. The results indicate that smaller tunnel cross-sections significantly affect ceiling temperature and smoke layer thickness, while larger cross-sections impact the smoke-control performance of the air curtain. Longitudinal wind speed strongly influences smoke propagation; a critical wind speed of 2.5 m/s is identified for suppressing upstream smoke backflow in this model. However, excessive wind speed can reduce downstream visibility, which can be compensated by increasing the suction flow rate. Ambient temperature and humidity also affect smoke diffusion and composition. The findings provide theoretical guidance for optimizing blowing–suction air curtain parameters and for analyzing complex tunnel fire scenarios.

1. INTRODUCTION

With the acceleration of urbanization in various countries and the continuous expansion of public infrastructure, global tunnel construction is trending toward larger cross-sections and extending to longer and deeper directions [1]. According to relevant reports, the total number of highway tunnels in China is approximately 28,300, with a total length exceeding 31,800 km. The total number of railway tunnels has exceeded 21,000, with a total length exceeding 25,000 km. Tunnels have become key road carriers to overcome terrain obstacles and connect different regions [2], while effectively shortening travel distances, alleviating traffic pressure [3], and avoiding damage to ecological balance. However, the closed and narrow structure of tunnels also brings fire safety challenges [4]. Tunnel fires have developed rapidly and have become one of the most concerning risks due to their high hazards and losses [5]. Tunnel fires produce high-temperature and highly toxic smoke, which is initially constrained by the accumulation of heat in confined spaces [6], and pose fatal dangers to personnel evacuation, structural safety, and rescue operations in a short time [7, 8]. Therefore, how to effectively prevent and control the hazards of tunnel fire smoke has become a key issue in the field of tunnel engineering. Tunnel cross-sectional size, tunnel slope, environmental pressure, ambient temperature and humidity, and natural longitudinal wind may affect key parameters such as fire source power, smoke propagation, ceiling temperature distribution, smoke layer height, and critical wind speed [9, 10], collectively influencing the development trend of fire dynamics.

Therefore, studying the effects of environmental factors on the smoke control capability of blowing–suction air curtains and providing theoretical references for tunnel fire safety is of great significance.

Many scholars have studied tunnel cross-sectional structure as a key influencing factor for tunnel fires. Yan et al. [11] focused on the effects of different tunnel cross-sectional sizes on flame height and temperature distribution, finding that tunnel height has little effect on flame behavior and temperature in the impact zone but has a larger effect on lateral temperature far from the fire source. Ji et al. [12] and others used a tunnel model with adjustable width to investigate the effects of tunnel width on mass loss rate, maximum smoke temperature, and temperature distribution below the ceiling. As the tunnel width decreased, the smoke temperature below the ceiling decayed more slowly in both longitudinal and lateral directions, while the mass loss rate and maximum smoke temperature were less affected. Tang et al. [13] established that by keeping the tunnel cross-sectional area constant and increasing the aspect ratio, the contact area between smoke and tunnel walls and surrounding cold air increases, leading to faster smoke temperature decay. At the same time, an empirical model was established to predict the maximum gas temperature rise and its longitudinal distribution. Liu et al. [14] introduced a sectional coefficient to describe tunnel cross-sectional geometric characteristics and used Fire Dynamics Simulator (FDS) to simulate nine different tunnel cross-sectional shapes to obtain predictive models for maximum smoke temperature and smoke temperature distribution. Longitudinal wind, as a major focus

in tunnel fire ventilation research in recent years, has also been extensively studied by domestic and international scholars. Wang et al. [15] set longitudinal wind speeds of 0–2 m/s, environmental pressures of 50–101 kPa, and fire source powers of 3 MW and 5 MW, and summarized that longitudinal wind gradually weakens the vertical and longitudinal distribution differences of carbon monoxide and smoke temperature, enhancing local smoke exhaust performance in shafts, but increasing wind speed reduces overall shaft smoke exhaust efficiency. Zhong et al. [16] studied tunnel fires under the combined effect of longitudinal ventilation and shaft chimney effect, and found that at higher longitudinal wind speeds, the driving force for smoke exhaust weakens and is accompanied by significant boundary layer separation, leading to a significant decrease in overall smoke exhaust capacity. Wu et al. [17] simulated the coupling of environmental wind conditions and shafts, summarizing that the larger the shaft size and the lower the environmental wind speed, the faster the temperature decay inside the tunnel, and established a dimensionless calculation model for the influence of environmental wind and shaft size. Li et al. [18] conducted experiments on uphill sloped tunnels under different boundary conditions, finding that the critical speed is jointly influenced by heat release rate and tunnel slope, estimating the ventilation pressure required for the tunnel to reach a critical state, and formulating effective longitudinal ventilation schemes. Jiao et al. [19] observed that increasing tunnel slope changes the oil fuel diffusion pattern, and the unit-area mass burning rate decreases under low ventilation speed (less than 0.5 m/s) while remaining basically stable under high ventilation speed, attributing this phenomenon to changes in flame tilt behavior under different ventilation conditions. Ma et al. [20] further studied two typical ignition conditions for multiple fire sources in tunnels under longitudinal ventilation, and for each critical ignition state, proposed a formula for predicting downstream smoke temperature rise. This study helps to understand the ignition process of multiple fire sources in tunnels. Scholars have also studied the effects of ambient temperature and humidity on tunnel construction and protection. Wang et al. [21] considered high-temperature and high-humidity environments as critical challenges for tunnel construction, establishing an experimental platform for internal tunnel ventilation cooling and dehumidification, analyzing the evolution of temperature and humidity under mechanical ventilation, and developing a deep learning model to predict the evolution of temperature and humidity in tunnel construction ventilation. Tao et al. [22] established a numerical heat transfer model for tunnels in cold regions and

found that mechanical ventilation can effectively reduce the area with internal tunnel temperatures below 0 °C, and that setting insulation layers can significantly extend the frost protection length of surrounding rock. In summary, scholars have studied the effects of tunnel cross-sectional size, longitudinal wind, and ambient temperature and humidity on tunnel fire safety, revealing the influence of environmental factors on fire source behavior, smoke temperature, and shaft smoke exhaust efficiency. Currently, there is limited research on tunnel fire smoke under blowing–suction air curtain scenarios by adjusting initial environmental parameters, and the interactions of various environmental factors can be further studied. Therefore, this study systematically investigates the effects of longitudinal wind and selected environmental factors on fire smoke behavior, temperature field changes, and safety evacuation standards at occupant height, which is an urgent need to advance existing fire ventilation design theory and develop precise smoke control by blowing–suction air curtains. It provides theoretical references to improve the resilience of tunnel fire safety protection.

2. FDS MODEL ESTABLISHMENT

2.1 Model parameters and operating conditions

In this study, the tunnel model is established using FDS. The model dimensions and related layout are shown in Figure 1. Tunnel model parameters are shown in Figure 2: the tunnel structural dimensions are divided into four types, namely 200 m × 10 m × 5 m, 200 m × 11 m × 7 m, 200 m × 12 m × 6 m, and 200 m × 14 m × 8 m. The tunnel walls are made of concrete with a density of 2280.0 kg/m³, specific heat of 1.04 kJ/(kg·K), thermal conductivity of 1.8 W/(m·K), and thickness of 0.1 m. The initial environmental temperature and humidity of the tunnel fire are set according to different operating conditions, and the environmental pressure is set to 0.1013 MPa. Both ends of the tunnel are set as “Open” to represent normal traffic conditions. The blowing–suction air curtain is set as a “Supply” curtain at the lower part of the tunnel and an “Exhaust” curtain at the upper part, with related parameters shown in the model figure. The twin fire sources are located in the center section of the tunnel, spaced 4 m apart, with dimensions of 4 m × 2 m × 1 m. The fuel is heptane with 7 carbon atoms and 16 hydrogen atoms, and the fire source adopts a transient ultra-fast fire. Measurement points are evenly arranged in different regions according to the research content for simulation monitoring.

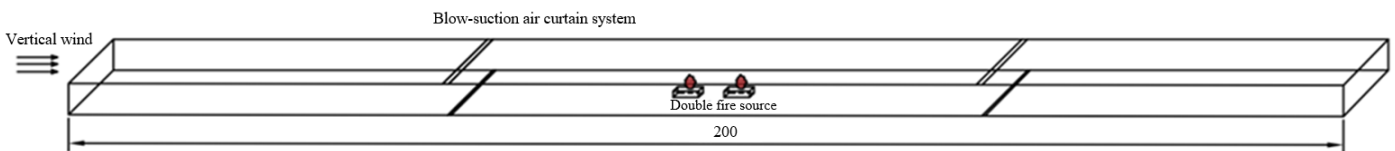


Figure 1. Tunnel model

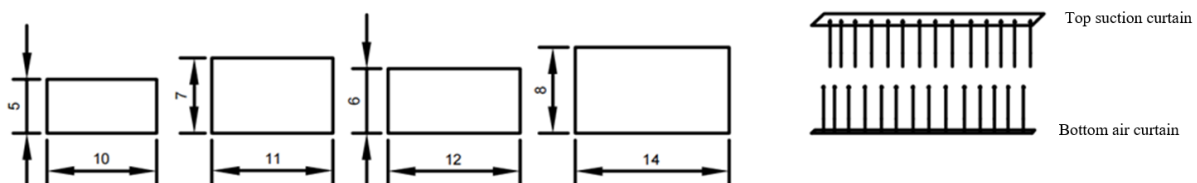


Figure 2. Cross-sectional dimensions of different tunnels and blowing–suction air curtain diagram

This study mainly analyzes the temperature distribution, horizontal smoke propagation, smoke layer height, and key safety indicators at a personnel characteristic height of 2 m by changing cross-sectional dimensions, longitudinal wind speed, initial environmental temperature, and humidity. The blowing

speed is constant at 2 m/s, and the suction speed is constant at 4 m/s, with subsequent adjustments according to simulation results. All simulation operating conditions are shown in Tables 1-4.

Table 1. Tunnel operating conditions with different cross-sectional dimensions

No.	Cross-sectional Size	Longitudinal Wind Speed	Ambient Temperature	Ambient Humidity
1	10 m × 5 m	0 m/s	20 °C	40%
2	11 m × 7 m			
3	12 m × 6 m			
4	14 m × 8 m			

Table 2. Tunnel operating conditions with different longitudinal wind speeds

No.	Cross-sectional Size	Longitudinal Wind Speed	Ambient Temperature	Ambient Humidity
5	10 m × 5 m	0 m/s	20 °C	40%
6		1 m/s		
7		1.5 m/s		
8		2 m/s		
9		2.2 m/s		
10		2.5 m/s		
11		3 m/s		

Table 3. Tunnel operating conditions with different ambient temperatures

No.	Cross-sectional Size	Longitudinal Wind Speed	Ambient Temperature	Ambient Humidity
12	10 m × 5 m	0 m/s	0 °C	40%
13			10 °C	
14			20 °C	
15			30 °C	
16			40 °C	

Table 4. Tunnel operating conditions with different ambient humidity

No.	Cross-sectional Size	Longitudinal Wind Speed	Ambient Temperature	Ambient Humidity
17	10 m × 5 m	0 m/s	20 °C	20%
18				40%
19				60%
20				80%
21				95%

2.2 Grid size rationality verification

The grid size in FDS simulation determines the accuracy of the simulation results; therefore, it is necessary to verify the grid rationality and select an appropriate grid size for simulation tests. Referring to the independent grid test results of McGrattan et al. [23], the ratio range between the fire characteristic diameter D^* and the grid size δ_x should be 4–16 for accurate calculation of the fluid viscous stress model. The relevant calculation formula for the fire characteristic diameter D^* is shown in Eq. (1):

$$D^* = \left(\frac{Q}{\rho_1 c_p T g^{1/2}} \right)^{2/5} \quad (1)$$

where, Q — fire power (kW); ρ — ambient density (kg/m³); c_p — specific heat at constant pressure (kJ/(kg·K)); g — gravitational acceleration (m/s²).

In this study, four different grid sizes of 0.167 m, 0.2 m, 0.333 m, and 0.5 m are selected for rationality verification. Taking a twin fire source of 10 MW as an example, the ceiling temperature above the twin fire source center is monitored

under different grid sizes. The temperature variation over time is shown in Figure 3.

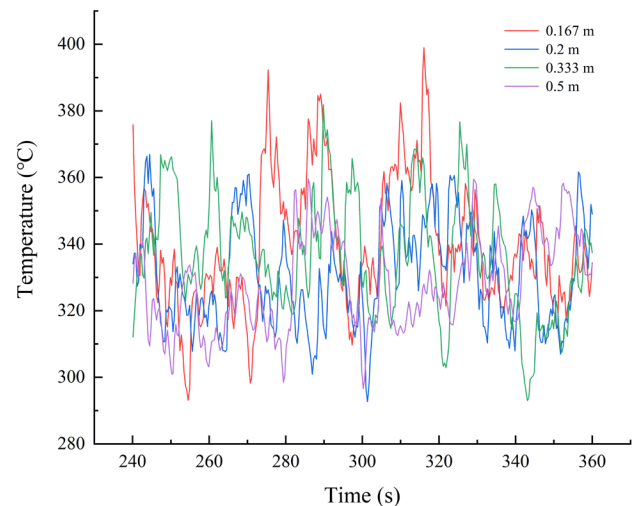


Figure 3. Steady-state combustion temperature variation at the ceiling center for different grid sizes under twin fire sources

The smaller the grid size, the smaller the fluctuation range and the more accurate the calculation. However, too small a grid size demands higher computer performance and longer computation time. Therefore, considering these factors, a grid size of 0.333 m is adopted for this simulation, and the simulation time is 360 s.

3. SIMULATION DATA PROCESSING AND RESULT ANALYSIS

3.1 Influence of different cross-sectional sizes on longitudinal ceiling temperature distribution and smoke propagation

From Figure 4, it can be observed that the smaller the tunnel cross-sectional size, the higher the maximum ceiling temperature and the longitudinal smoke temperature. This fully indicates that tunnel cross-sectional size can significantly affect the longitudinal distribution of smoke and the impact on the ceiling structure. For the smallest cross-section of 10 m × 5 m, the temperature peak directly above the twin fire sources is 782 °C, which is approximately 448 °C higher than the largest cross-section of 14 m × 8 m. Due to the tunnel being a confined space, the high-temperature smoke generated by the fire is restricted in a smaller space, forming local vortices and accumulating near the tunnel ceiling to create a thicker and hotter high-temperature smoke layer. In addition, the entrainment effect of hot smoke is weakened in the upward process due to the limited space, which may lead to higher flame and smoke temperatures. The nearby sidewalls and ceiling also generate radiative heat feedback, further increasing the ceiling temperature. The smoke volume generated by the same fire power is roughly the same. In large cross-section tunnels, the flow cross-sectional area of the smoke layer is larger, the longitudinal smoke velocity is lower, and the smoke has more time to exchange heat with the surrounding air. As the distance increases, the temperature difference between the ceiling and the smoke causes the longitudinal smoke temperature to decrease rapidly, forming a relatively stable decay pattern.

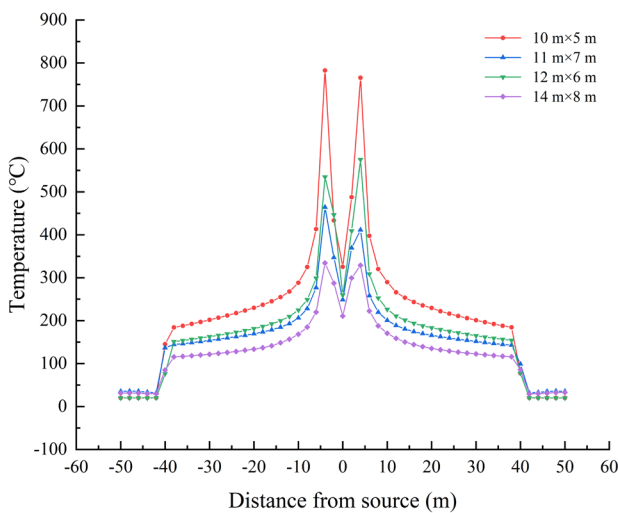


Figure 4. Longitudinal ceiling temperature distribution for different cross-sectional sizes

From Figure 5, it can be seen that the blowing–suction air curtain in tunnels with different cross-sectional sizes has

different smoke control performance. The air curtain with blowing speed of 2 m/s and suction speed of 4 m/s can effectively control smoke flow for cross-sectional sizes of 10 m × 5 m and 12 m × 6 m. When the cross-sectional area increases, some smoke leakage occurs for 11 m × 7 m and 14 m × 8 m. The jet from the blowing port forms an air curtain wall; its vertical momentum counteracts the horizontal propagation of smoke, and the vertical suction from the suction port prevents smoke diffusion. The vertical distance that the jet needs to cover increases, and by the time it reaches the upper part of the tunnel and converges with the suction curtain, its velocity has decayed significantly, failing to form an effective seal. In large-size tunnels, turbulence caused by fire is more complex and easily disturbs the relatively fragile air curtain jet, disrupting its stability and causing gaps in the flow field. The air curtain itself occupies part of the tunnel flow area, creating local blockage. In smaller cross-section tunnels, the blocking effect of the air curtain is significant, enhancing the pressure difference and flow rate upstream and downstream, requiring a balance between smoke control and ventilation resistance. In large cross-section tunnels, the blocking ratio of the air curtain is relatively small, and the disturbance to the overall flow field is less, but its momentum must overcome the larger volume of tunnel main airflow. From Figure 6, increasing the suction speed of the air curtain for heights of 7 m and 8 m improves smoke control. Timely removal of smoke blocked and cooled by the air curtain prevents accumulation in front of the curtain, maintaining curtain integrity. This indicates that the blowing–suction air curtain has an adapted blowing–suction speed parameter as the minimum standard for smoke control for different cross-sectional sizes. Tunnels with larger cross-sections require faster blowing–suction speeds or larger blowing–suction port sizes, or an additional set of air curtains with smaller parameters as auxiliary measures.

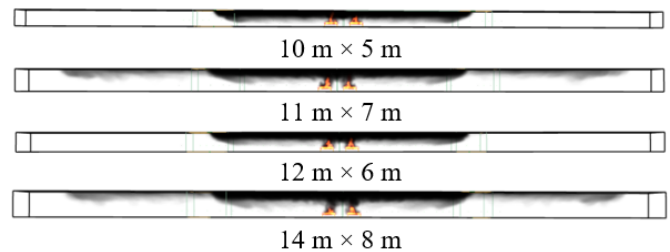


Figure 5. Smoke control for different cross-sectional sizes with suction speed of 4 m/s

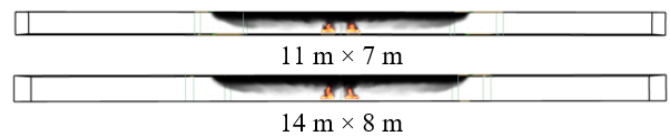


Figure 6. Smoke control for different cross-sectional sizes with suction speed of 8 m/s

3.2 Influence of different tunnel cross-sectional sizes on smoke layer height

From Figure 7, it can be seen that the cross-sectional height difference in the tunnel plays a dominant role, and the smoke layer distribution is relatively obvious. The higher the size height, the lower the smoke layer height. However, after removing the size height difference for relative comparison,

the larger the cross-sectional height, the lower the smoke layer height. Under the same smoke generation rate, the smaller the spatial volume, the weaker the dilution capacity. The contact area between smoke and tunnel walls is large, and friction resistance is high. This hinders rapid longitudinal transport of smoke, causing smoke to accumulate more easily near the fire source area, thereby filling the section faster, showing a faster local smoke layer height decline. Due to the large cross-sectional size, the smoke temperature decreases, so the comparison of smoke layer height after removing height difference shows that larger cross-sectional size leads to lower smoke temperature, reduced buoyancy, and inability to maintain a high position, naturally causing smoke to sink or be more easily dispersed by airflow. Therefore, the smoke layer height is lower. Comparing smoke layer heights, tunnels with smaller cross-sectional sizes pose greater danger to personnel evacuation safety during fires (Figure 8).

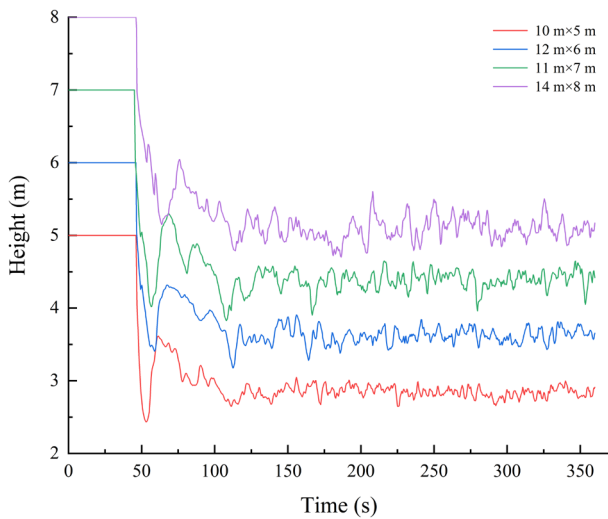


Figure 7. Smoke layer height for different cross-sectional sizes

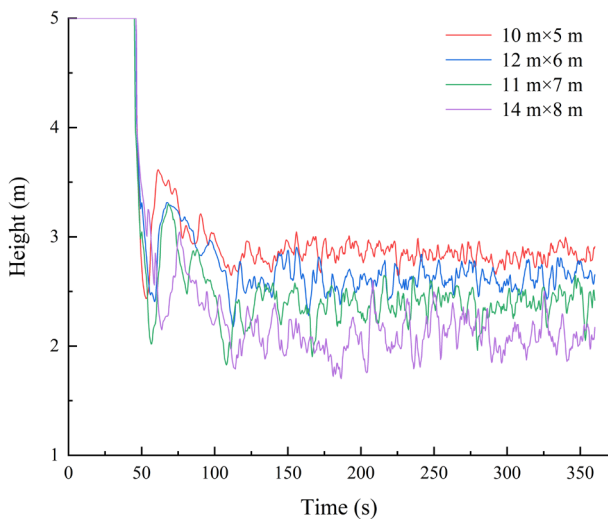


Figure 8. Comparison of smoke layer height after removing size height difference

3.3 Influence of different longitudinal wind speeds on smoke backflow length

From Figure 9, it can be observed that increasing longitudinal wind speed can reduce smoke backflow length,

hindering the horizontal spread of smoke upstream, and providing a longer safe space for personnel evacuation. When the wind speed is 0 m/s, smoke generated by the fire source spreads toward the upstream exit without the control of the blowing–suction air curtain. When the wind speed increases to 1.5 m/s, the longitudinal wind kinetic energy is significantly enhanced, beginning to suppress the smoke thermal buoyancy, and the backflow length decreases sharply. Natural wind speed may stabilize between 1.0–2.5 m/s. At this stage, natural wind is the dominant wind speed, and smoke control in tunnel fires may be most unfavorable, with a longer backflow length, posing a high threat to the upstream. It is necessary to start jet fans to increase wind speed to suppress backflow. When the wind speed reaches 2.5 m/s, smoke above the twin fire sources no longer spreads upstream, and the longitudinal wind reaches the critical wind speed. When the longitudinal wind speed continues to increase, smoke backflow may completely disappear, converting to fully downstream diffusion. Longitudinal wind speed of 2.5 m/s synergistically enhances the effect of the blowing–suction air curtain. The momentum of longitudinal wind and the air curtain couples to form stronger blocking and entrainment effects, achieving the optimal coupling state. Subsequently, increasing the suction speed to 10–12 m/s allows the blowing–suction air curtain to effectively control smoke generated both upstream and downstream, mainly analyzing key indicators such as visibility at downstream personnel characteristic height to test the coupling effect of longitudinal wind and the air curtain.

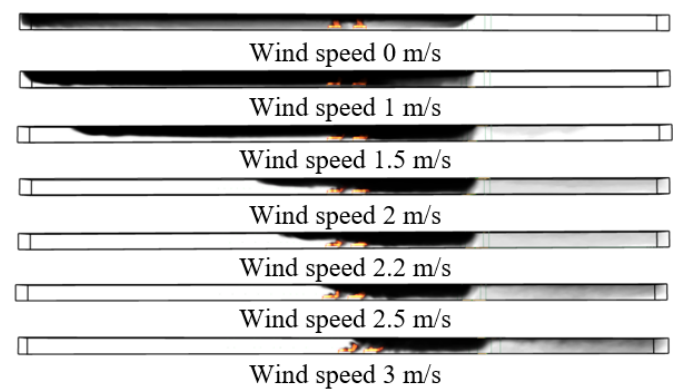


Figure 9. Backflow length under different longitudinal wind speeds

3.4 Influence of different longitudinal wind speeds on ceiling temperature distribution and downstream non-protected personnel visibility

From Figure 10, it can be seen that the coupling of different longitudinal wind speeds and the blowing–suction air curtain has a significant effect on reducing ceiling temperature. When there is no longitudinal wind, the ceiling temperature above the twin fire sources reaches 759 °C, the highest temperature in the condition, with slow temperature decay. When longitudinal wind speed is 1–3 m/s, as the wind speed increases, the ceiling smoke temperature decreases sharply. With increasing longitudinal wind speed, the high-temperature smoke generated by the fire source is blown downstream, reducing the residence time of smoke above the twin fire sources. Therefore, the ceiling near the fire source is no longer continuously heated, and the ceiling temperature significantly decreases. Under larger natural or mechanical ventilation speeds, the turbulence intensity of smoke flow increases,

enhancing the mixing and heat exchange between smoke and nearby cold air, and convective heat transfer with tunnel walls increases. Longitudinal wind tilts the flame toward the right-side fire source, causing the temperature on the right side to be higher than on the left side. When the wind speed reaches 3 m/s, the longitudinal ceiling temperature distribution in the downstream section is about 135 °C, which has little effect on the tunnel top structure. Under coupling, the high-temperature area not only has a lower peak but also a lower average longitudinal temperature, and the smoke layer temperature is more uniform, enabling more efficient ventilation and smoke exhaust during twin fire source fires.

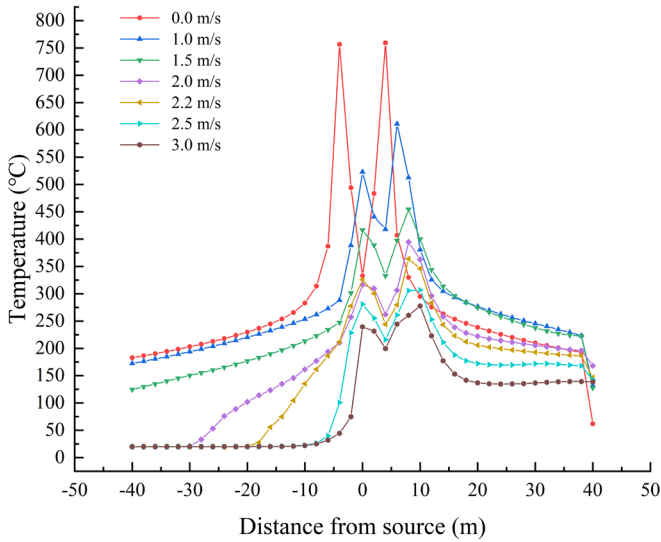


Figure 10. Ceiling temperature changes under different longitudinal wind speeds

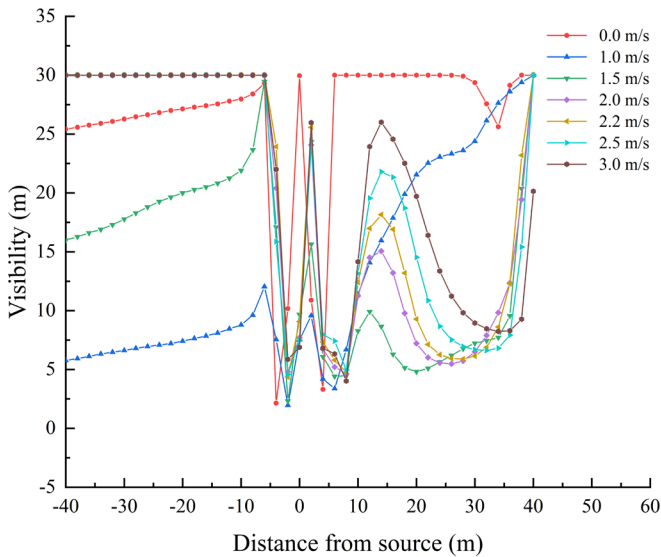


Figure 11. Visibility changes under different longitudinal wind speeds

From the data shown in Figure 11, the visibility of personnel on the left side is very high, while the visibility of personnel on the right side is lower. With the effect of longitudinal wind, visibility on both sides gradually increases. Without longitudinal wind, the left-side visibility is high because the tunnel model is short, and smoke is discharged from the exit without timely settling. In an actual long tunnel, smoke would spread to the lower part of the tunnel, affecting personnel

visibility. The right side is controlled and discharged by the blowing–suction air curtain, not affecting visibility. Visibility is one of the key indicators to measure the effectiveness of smoke control by the air curtain. This figure provides a simulation basis for determining optimal longitudinal wind speed and air curtain parameters. From the figure, when the wind speed is above 1.5 m/s, upstream visibility above the fire source is about 30 m, indicating low smoke spread upstream. The higher the longitudinal wind speed, the stronger the turbulence formed by the coupling of the air curtain and wind, drawing more fresh air into the smoke layer, significantly diluting smoke particle concentration and improving visibility. When visibility is below 10 m, changes in longitudinal wind mainly affect downstream personnel visibility. The longitudinal wind carries upstream smoke downstream, restricting smoke in the downstream tunnel section. At this time, the blowing–suction air curtain cannot discharge smoke in time, reducing downstream personnel visibility. Although increasing wind speed can effectively improve visibility, the maximum wind speed of 3 m/s still does not fully achieve 10 m. This coupling ensures safety for upstream personnel evacuation but does not increase the safe distance for downstream personnel evacuation. By increasing the suction speed to 12 m/s, the control and discharge of twin fire source smoke by the blowing–suction air curtain are strengthened, providing a downstream evacuation area with visibility greater than 10 m.

3.5 Influence of different environmental temperatures on smoke layer height during steady-state combustion

Figure 12 shows the actual smoke layer height in the tunnel after reaching steady-state combustion, extracted from 315–360 s, simulated using FDS with initial tunnel environmental temperature set to 0 °C, 10 °C, 20 °C, 30 °C, and 40 °C. Simulation results indicate that smoke layer height shows a positive correlation with environmental temperature. Under 0 °C and 10 °C conditions, the smoke layer height is relatively low, with a thicker smoke layer, while at 30 °C and 40 °C, the steady-state smoke layer height is relatively high, and the smoke layer thickness is thinner. The core driving force for smoke layer formation originates from buoyancy effects caused by the density difference between the fire plume and surrounding air due to temperature differences. According to the ideal gas equation of state, environmental air density is inversely proportional to environmental temperature. When the twin fire source power is constant, the average temperature of the plume and the smoke density can be approximated as constant. Therefore, with increasing environmental temperature, the environmental air density decreases, reducing the density difference between smoke and surrounding air. This means the initial buoyancy flux is weakened. Reduced buoyancy slows the plume rise velocity, and the entrainment rate is positively proportional to the plume rise velocity. In a high-temperature environment, the amount of cold air entrained into the plume and subsequently becoming part of the smoke layer decreases, leading to a reduction in total smoke volume flow. Under the same ceiling jet spreading and settling effect, at higher environmental temperatures, the strong buoyancy drives smoke to rise rapidly and cling to the ceiling, forming a stable thin smoke layer. Conversely, in a low-temperature environment, strong buoyancy drives vigorous entrainment, generating a large amount of low-temperature diluted smoke, which sinks and accumulates,

forming a thicker smoke layer.

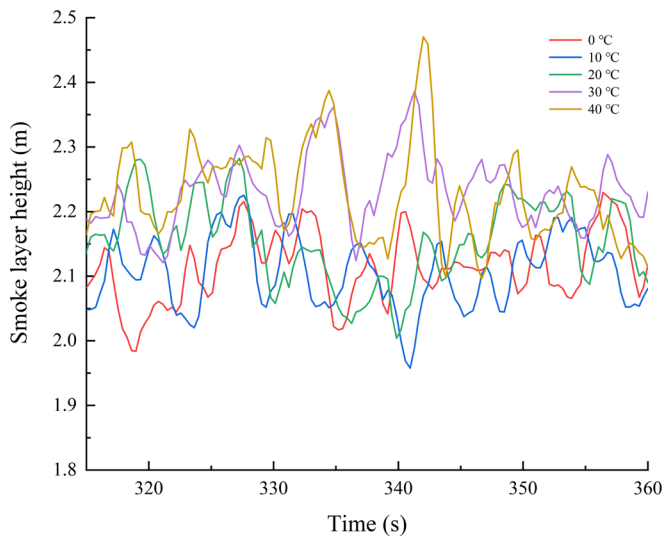


Figure 12. Smoke layer height under different environmental temperatures from 315–360 s

3.6 Influence of different environmental temperatures and humidities on vertical temperature

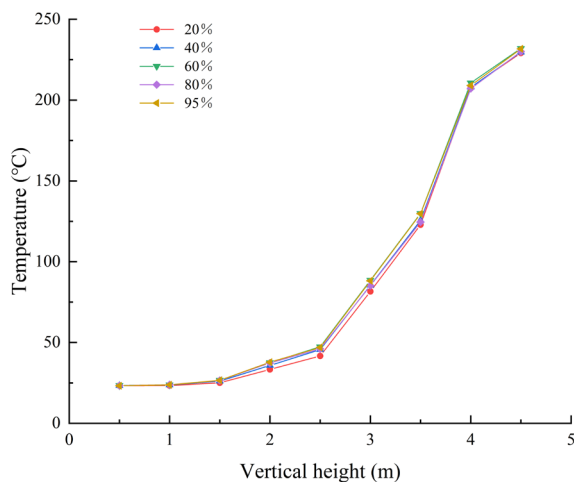


Figure 13. Vertical temperature under different environmental humidities

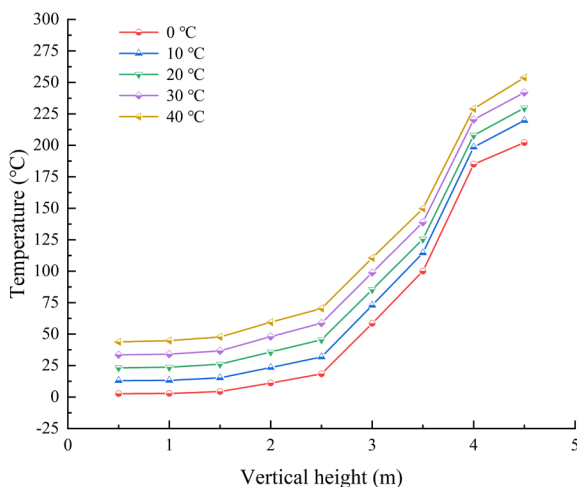


Figure 14. Vertical temperature under different environmental temperatures

According to Figures 13 and 14, the vertical temperature distribution in the tunnel forms a typical thermal stratification structure. All curves show similar increasing trends. At ceiling height (4.9 m), under 0 °C condition, the smoke layer temperature is approximately 202 °C, while under 40 °C condition, it rises to approximately 253 °C. Data indicate that the vertical temperature difference is approximately equal to the initial environmental temperature difference. The environmental temperature increase not only shifts the baseline but also increases the absolute temperature rise of the smoke layer. At personnel height near the tunnel floor (< 2 m), under low-temperature condition (0 °C), the low-temperature environment near 0 °C can still be maintained, while under high-temperature condition (40 °C), the temperature at this vertical height reaches approximately 60 °C. During fires in winter or cold environments, a cold air layer exists at the floor for evacuation, whereas in summer or hot environments, fire rapidly heats the entire tunnel space to dangerous temperatures from the initial high temperature. Comparing different environmental temperatures and humidities, it is found that environmental humidity has a minor effect on vertical smoke temperature, with low humidity slightly reducing smoke temperature. In contrast, environmental temperature mainly affects the overall smoke temperature according to the initial temperature difference. These two boundary conditions affect the vertical temperature distribution of smoke in two forms.

3.7 Influence of different environmental temperatures on transverse temperature

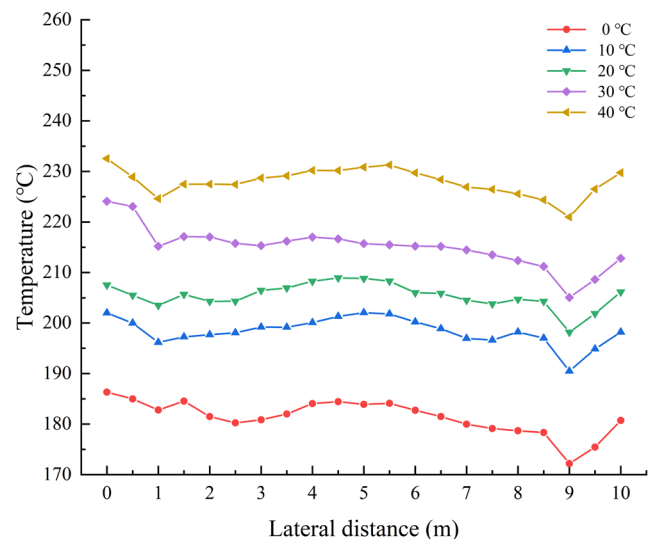


Figure 15. Transverse temperature under different environmental temperatures

From Figure 15, as the initial environmental temperature increases from 0 °C to 40 °C, the entire transverse temperature distribution curve shifts upward along the vertical coordinate. The ceiling temperature under 40 °C condition is approximately 60–70 °C higher than that under 0 °C, and this increase is significantly greater than the environmental temperature difference. Under lower environmental temperatures, high-temperature zones are concentrated near the fire source axis and at the tunnel transverse ends. Under higher environmental temperatures, the peak temperature region significantly widens, and the top of the curve becomes flatter, indicating that high-temperature smoke diffuses more uniformly under the ceiling. During the transverse spread of

ceiling jets, heat is continuously lost through convective heat transfer with the ceiling walls and radiative and convective heat transfer with the underlying cold air layer. The heat transfer rate strongly depends on the temperature difference. At high environmental temperatures, buoyancy weakens, and secondary flows and turbulence pulsation driven by buoyancy are suppressed, while mechanical diffusion relatively increases. This causes heat diffusion in the transverse direction to rely more on gentle shear layer mixing rather than strong buoyancy-driven entrainment, forming a more uniform transverse temperature field.

3.8 Influence of different environmental humidities on CO concentration at personnel characteristic height in non-protected zones

Figure 16 shows the CO concentration distribution at 2 m height in the fire source section from 90–110 m under different initial environmental humidities. In all conditions, the lower the environmental humidity, the higher the overall CO concentration level and peak value. Initial environmental humidity is a key chemical boundary condition affecting CO concentration distribution in tunnel fires. In low-humidity environments, the water vapor content in the air is low, resulting in a dry atmosphere, which significantly reduces the generation of OH radicals in the high-temperature fire zone. This prevents CO from being oxidized into CO₂ in time, causing it to accumulate in the smoke. In tropical, subtropical coastal tunnels or underwater tunnels, the environment may exceed 90% relative humidity. In high-humidity tunnel fire environments, the fundamental reason for increased CO concentration is that excess water vapor acts as a strong heat sink and diluent, significantly reducing flame temperature and deteriorating local oxygen concentration, pushing the combustion state toward a low-temperature, oxygen-deficient incomplete combustion region, thereby producing a large amount of CO. Except for the CO concentration at the twin fire source location, the overall CO concentration level remains below 50×10^{-6} ppm.

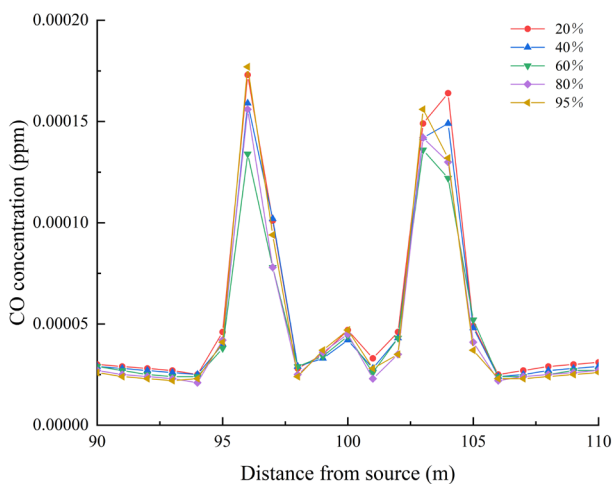


Figure 16. CO concentration under different environmental humidities

4. CONCLUSIONS

In response to the comprehensive development of modern tunnels, this study established a model and conducted scenario

tests using the fire dynamics simulation software FDS. The study analyzed the influence of different tunnel cross-sectional sizes, longitudinal wind speeds, and environmental temperature and humidity on fire smoke characteristics under the scenario of a twin-fire source with a blow-suction air curtain. The main conclusions are as follows:

(1) Among the four tunnel cross-sectional size conditions, smaller cross-sectional sizes intensify the fire smoke effects: higher ceiling temperatures, thicker smoke layers, and faster downward accumulation, posing greater threats to personnel evacuation safety and tunnel structural safety. Furthermore, tunnel cross-sectional size affects the smoke control effectiveness of the blow-suction air curtain. When the cross-sectional width ≥ 7 m, the suction air curtain velocity needs to be increased from 4 m/s to 8 m/s to enhance smoke blocking and removal.

(2) From the study of different longitudinal wind speed conditions, a longitudinal wind speed of 2.5 m/s on the left side reaches the critical wind speed for effectively suppressing smoke upstream in this tunnel model. The greater the longitudinal wind speed, the smaller the longitudinal ceiling temperature distribution of the twin fire sources. When longitudinal wind speed exceeds 1.5 m/s, smoke leakage occurs on the right-side blow-suction air curtain, reducing visibility at 2 m height in the downstream non-protected zone to less than 10 m. By increasing the suction velocity to 12 m/s, the spread of smoke to the downstream protected zone can be effectively controlled.

(3) Environmental temperature and humidity, as the initial boundary conditions of this simulation, were found to significantly affect smoke behavior. Environmental temperature mainly alters the thermal buoyancy effect of smoke; higher temperatures result in higher smoke layers, while lower temperatures produce thicker smoke layers. The vertical and transverse temperature distributions under different environmental temperatures are mainly determined by the initial temperature difference, with summer or hot regions having a greater impact on smoke temperature. Environmental humidity influences CO generation through chemical reactions in fire smoke; excessive humidity cools the flame and promotes incomplete combustion, increasing the risk of smoke toxicity.

Based on this simulation, further research will use orthogonal analysis to comprehensively study the coupling effects of environmental factors on fire smoke characteristics and fire source behavior. Comparative studies will determine the optimal blow-suction air curtain parameters for smoke blocking and removal, followed by in-depth study of multi-fire source scenarios.

REFERENCES

- [1] Fan, L., Ma, W., Tao, L., Yuan, Y., Zeng, Y., Chen, H. (2025). Ambient temperature field and energy consumption analysis of air channel construction ventilation in high-geotemperature tunnels. *Applied Thermal Engineering*, 274: 126844. <https://doi.org/10.1016/j.applthermaleng.2025.126844>
- [2] Chen, L., Li, J., Zhang, Y., Han, F., Ji, C., Zhang, J. (2019). Study on coupled heat transfer and seepage in large sparsely fractured surrounding rocks in deep underground spaces. *Applied Thermal Engineering*, 162: 114277.

- <https://doi.org/10.1016/j.applthermaleng.2019.114277>
- [3] Wan, H., Liu, T., Yu, H., Zhang, Y., Li, T. (2026). Research on longitudinal ceiling gas temperature of two fires with unequal heat release rates in a high-altitude tunnel under natural ventilation. *Tunnelling and Underground Space Technology*, 168: 107205. <https://doi.org/10.1016/j.tust.2025.107205>
- [4] Hu, P., Zhong, M., Cheng, H., Chen, J., Zhang, P. (2025). Temperature decay and heat exhaust efficiency under ceiling multi-point centralized smoke exhaust in a ventilated tunnel. *Tunnelling and Underground Space Technology*, 163: 106658. <https://doi.org/10.1016/j.tust.2025.106658>
- [5] Wu, P., Chi, J., Zhou, R., Hao, M., Jiang, J. (2025). Numerical simulations and theoretical analysis of ambient wind impact on shaft smoke exhaust performance in tunnel fires. *Tunnelling and Underground Space Technology*, 166: 106975. <https://doi.org/10.1016/j.tust.2025.106975>
- [6] Sun, C., Weng, M., Liu, F., Yang, H., Du, K., Lei, X. (2026). Fire source elevation effects on smoke transport in inclined tunnels: Scaled experiments, synergistic mechanisms, and predictive model enhancements. *Tunnelling and Underground Space Technology*, 168: 107146. <https://doi.org/10.1016/j.tust.2025.107146>
- [7] Ji, J., Wang, Z., Ding, L., Yu, L., Gao, Z., Wan, H. (2019). Effects of ambient pressure on smoke movement and temperature distribution in inclined tunnel fires. *International Journal of Thermal Sciences*, 145: 106006. <https://doi.org/10.1016/j.ijthermalsci.2019.106006>
- [8] Wan, H., Gao, Z., Ji, J., Fang, J., Zhang, Y. (2019). Experimental study on horizontal gas temperature distribution of two propane diffusion flames impinging on an unconfined ceiling. *International Journal of Thermal Sciences*, 136: 1-8. <https://doi.org/10.1016/j.ijthermalsci.2018.10.010>
- [9] Tang, F., He, Q., Mei, F., Shi, Q., Chen, L., Lu, K. (2018). Fire-induced temperature distribution beneath ceiling and air entrainment coefficient characteristics in a tunnel with point extraction system. *International Journal of Thermal Sciences*, 134: 363-369. <https://doi.org/10.1016/j.ijthermalsci.2018.08.023>
- [10] Ji, J., Guo, F., Gao, Z., Zhu, J., Sun, J. (2017). Numerical investigation on the effect of ambient pressure on smoke movement and temperature distribution in tunnel fires. *Applied Thermal Engineering*, 118: 663-669. <https://doi.org/10.1016/j.applthermaleng.2017.03.026>
- [11] Yan, W., Li, C., Zhao, P., An, H., Gao, Z. (2025). Experimental investigation on the impact of cross-section dimensions on the thermal properties of the ceiling flame impingement in tunnel fires. *International Communications in Heat and Mass Transfer*, 161: 108529. <https://doi.org/10.1016/j.icheatmasstransfer.2024.108529>
- [12] Ji, J., Bi, Y., Venkatasubbaiah, K., Li, K. (2016). Influence of aspect ratio of tunnel on smoke temperature distribution under ceiling in near field of fire source. *Applied Thermal Engineering*, 106: 1094-1102. <https://doi.org/10.1016/j.applthermaleng.2016.06.086>
- [13] Tang, Z., Gao, K., Tao, C., Liu, Y., Qi, Z. (2024). The influence of tunnel aspect ratio on the gas temperature distribution in advancing tunnel. *Tunnelling and Underground Space Technology*, 149: 105818. <https://doi.org/10.1016/j.tust.2024.105818>
- [14] Liu, F., Yu, L. X., Weng, M. C., Lu, X. L. (2016). Study on longitudinal temperature distribution of fire-induced ceiling flow in tunnels with different sectional coefficients. *Tunnelling and Underground Space Technology*, 54: 49-60. <https://doi.org/10.1016/j.tust.2016.01.031>
- [15] Wang, J., Kong, X., Fan, Y., Jiang, X., Lu, K. (2022). Reduced pressure effects on smoke temperature, CO concentration and smoke extraction in tunnel fires with longitudinal ventilation and vertical shaft. *Case Studies in Thermal Engineering*, 37: 102311. <https://doi.org/10.1016/j.csite.2022.102311>
- [16] Zhong, W., Fan, C. G., Ji, J., Yang, J. P. (2013). Influence of longitudinal wind on natural ventilation with vertical shaft in a road tunnel fire. *International Journal of Heat and Mass Transfer*, 57(2): 671-678. <https://doi.org/10.1016/j.ijheatmasstransfer.2012.10.063>
- [17] Wu, P., Wen, Z., Zhong, H., Zhou, R., Hao, M., Jiang, J. (2025). Influence of ambient wind on temperature distribution and smoke propagation in urban road tunnels with vertical shafts during fires. *Tunnelling and Underground Space Technology*, 166: 106983. <https://doi.org/10.1016/j.tust.2025.106983>
- [18] Li, P., Shang, L., Yang, D., Zhang, W. (2025). Experimental study and modelling on critical velocity, smoke temperature distribution and driving force in uphill tunnel fire with longitudinal ventilation. *Fire Safety Journal*, 160: 104604. <https://doi.org/10.1016/j.firesaf.2025.104604>
- [19] Jiao, W., Chen, C., Lin, Z., Bao, Y., Shi, L. (2024). Experimental study on the effect of longitudinal ventilation on spill fire characteristics in sloped tunnels. *International Journal of Thermal Sciences*, 206: 109269. <https://doi.org/10.1016/j.ijthermalsci.2024.109269>
- [20] Ma, Q., Chen, J., Chen, Z. (2025). Experimental study on the effect of longitudinal ventilation on the ignition characteristics of fires with multiple ignition sources in tunnels. *Applied Thermal Engineering*, 278: 127201. <https://doi.org/10.1016/j.applthermaleng.2025.127201>
- [21] Wang, S., Huang, F., Jiang, S., Yang, D., Zheng, A., Hu, Z. (2025). Evolution and prediction of temperature-humidity in hot-humid tunnels: experiments and machine learning. *Tunnelling and Underground Space Technology*, 165: 106869. <https://doi.org/10.1016/j.tust.2025.106869>
- [22] Tao, L., Tian, X., Zhou, X., Zeng, Y. (2022). Influence of mechanical wind heated by ground temperature on ambient temperature in tunnels: Numerical modeling, case study and analysis. *International Journal of Thermal Sciences*, 176: 107497. <https://doi.org/10.1016/j.ijthermalsci.2022.107497>
- [23] McGrattan, K., Hostikka, S., McDermott, R., Floyd, J., Weinschenk, C., Overholt, K. (2013). *Fire Dynamics Simulator User's Guide*. NIST Special Publication, Sixth Edition.